Effects of Reciprocation Number on the Friction Behaviors of Carbon/Epoxy for Various Fiber Orientations and High Contact Pressures

Shunsuke MATSUNAGA [1], Terutake MATSUBARA [2],
Wen-Xue WANG [2] and Yoshihiro TAKAO [2]
[1] *Graduate Student, Kyushu-University, 6-10-1, Hakozaki, Fukukoa 812-8581,Japan*
[2] *Kyushu-U, 6-1, Kasuga-koen, Fukuoka 816-8580, Japan*

SUMMARY: Coefficient of Friction of CFRP under a critically high contact pressure is investigated. To carry out this study, a frictional test apparatus which utilizes a conventional material test machine with hydraulic wedge grips was newly designed and its capability is verified. It is proved that this apparatus can measure the frictional force, where the coefficient of friction μ is smaller than nearly $tan\theta$ with θ as a wedge angle. Frictional experiments are conducted between CFRP and SUS under 150MPa to 375MPa. The μ then ranges 0.06 to 0.26 and the effects of fiber orientation α are obtained at each cycle. The μ increases almost monotonously with reciprocation number increasing at all fiber orientation angles, but the mechanism for α=0 ° is singular, where carbon fibers are easily damaged and worn out and consequently the surface fraction of epoxy is large at the frictional contact area. In other fiber orientation for $\alpha \neq$ 0 ° adhesion of worn materials to its counter part, that is , SUS occurs, and it seems to cause the increase of μ. Also there can be seen the effects of pressure, regardless of small numerical difference of coefficients of friction. Observation with an optical microscope and EPMA is performed and the mechanism for the increase of μ with cycle is considered.

KEYWORDS: CFRP, Friction, High contact pressure, Fiber orientation

INTRODUCTION

Carbon fiber reinforced plastics, CFRP, have been widely used. To build a structure it is inevitable to include some kinds of joints in the structure and its strength strongly depends on the mechanical behavior of joints. Mechanical fastened joints have been frequently used not only for conventional structural metals material but also for composite materials. However, damage initiate and propagate mechanism of the composite materials are fundamentally different from structural metals and extremely complex. Three failure modes of mechanical joints failure are well known such as shear-out, net-tension and bearing mode. Shear-out and net-tension failure modes can be predicted relatively easily by the two-dimensional structural analysis. But the bearing failure mode where the three-dimensional effect is dominant, can not be predicted appropriately by the two-dimensional analysis without considering the stacking sequences and stress distribution through the thickness direction.

Many analytical and experimental studies[1] have been performed for this bearing failure of mechanical fastened joints. The hole edge of CFRP has various shapes of fiber cross section, that is the fiber orientation is not the same with respect to the hole edge. The fiber orientation

angle changes continuously along the circumference direction and discretely along through the thickness direction. It is well known that the friction at the pin-hole edge has considerable effects on the bearing failure and it is necessary to study the relationship between the coefficient of friction and fiber orientation angle sufficiently under a critically high contact pressure.

Under a relatively low contact pressure, T.Tukizoe and N.Ohmae[2] measured a coefficient of friction of carbon and other several kinds of fiber reinforced plastic for three different sliding directions, i.e. parallel, anti-parallel and normal directions. Y.Xiao et al.[3] obtained the coefficient of friction experimentally as a function of fiber orientation and they[4] proposed a modified rule of mixture based on the classical lamination theory for coefficient of friction to a CFRP composite laminate edge. But their coefficients were obtained at a low contact pressure much smaller than failure stress of composite materials. To evaluate effects of friction on the bearing failure of a pinned-joint appropriately, a friction tester recently developed under a high contact pressure is discussed in detail and the effects of reciprocation number of sliding, contact pressure and fiber orientation are studied.

It should be mentioned that in recent years the field of tribology has received an increasing attention from the scientific, technical and practical points of view. It seem to be demanded that the tribological behavior of advanced composite materials is understood clearly.

EXPERIMENTAL

Friction Tester

Fig. 1 Experimental Setup

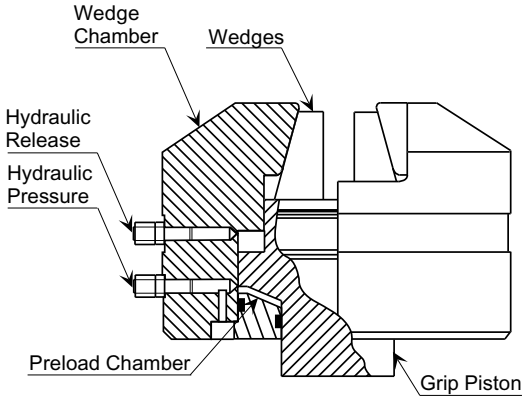

Fig. 2 Grip Cut-way View

This subsection deals with a new apparatus for the frictional experiment under a high contact pressure and the verification of its capability. Even for a 1cm^2 section specimen several tons of load is necessary to press CFRP up to the critical compressive pressure. Therefore, it seems to be no longer feasible to yield a high contact pressure by applying dead weight on a specimen for measuring the friction force. A newly designed friction tester system for this study adapts gripping force provided by hydraulic wedge grips of a material test machine in order to apply large contact force to the specimen. A conventional hydraulic material test machine supplies sliding force easily which is controlled and monitored, and the cyclic frictional test can be carried out without any additional complicated jig or preparation.

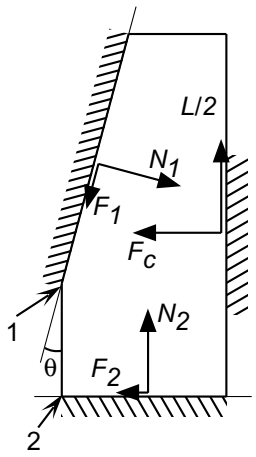

Fig. 3 Balance of Wedge

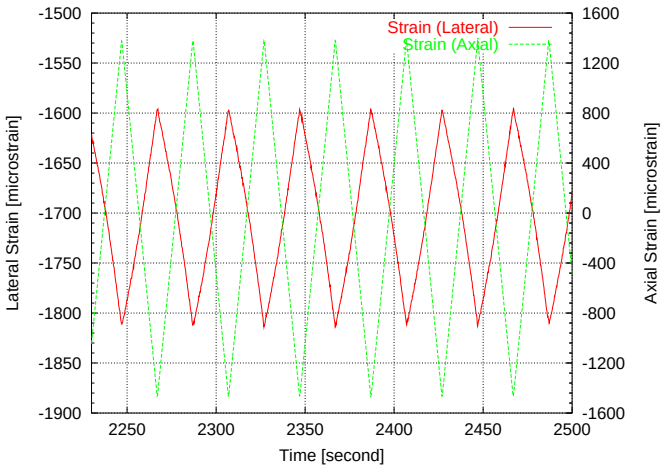

Fig. 4 Verification of contact force

Photographs of this new tester system is shown in Fig.1 later in Fig.5. Fig. 2 illustrates the mechanism of grip with hydraulic pressure at the preload chamber. As can be seen in Fig.3 a wedge contacts on three surfaces and several forces are applied through them. Assuming that coefficients of friction between the wedge and the wedge chamber or grip piston are the same μ_w, each friction force can be write as

$$F_1 = \mu_w N_1 \quad \text{and} \tag{1}$$
$$F_2 = \mu_w N_2 \tag{2}$$

Now considering that a downward force F_H which is produced by hydraulic pressure in the preload chamber is identical to the vertical component of the resultant of N_1 and F_1 acting to the wedge through the surface 1,

$$F_1 cos\theta + N_1 sin\theta = F_H/2, \tag{3}$$

which leads to

$$N_1 = \frac{F_H}{2(sin\theta + \mu_w cos\theta)} \tag{4}$$

Furthermore, the vertical and horizontal balance of the wedge yields

$$N_2 = \frac{F_H - L}{2} \quad \text{and} \tag{5}$$
$$F_c = \frac{F_H}{2}\left(\frac{cos\theta - \mu_w sin\theta}{sin\theta + \mu_w cos\theta}\right) - \frac{\mu_w (F_H - L)}{2}, \tag{6}$$

where L,F_c and θ denote an axial load of this material test machine, contact force applied to the specimen and wedge angle, respectively. According to the product manual of the present material test machine[5], μ_w is as small as 0.06.

F_c could be varied in certain range due to L included in the last term of eq.(6). The magnitude of L is nearly half of F_H and $(cos\theta - \mu_w sin\theta)/(sin\theta + \mu_w cos\theta)$ is 3. Thus, the effect of the practical variation of L on F_c is about $(0.06/3) \times (1/2)$, that is 1%. Therefore, as long as

Table 1 Test condition

Batch	N	SUS	CFRP
1	50	No Treatment	polished by #1500
2	100	No Treatment	polished by #1500
3	100	No Treatment	polished by #1500
4	15	polished by #2000	polished by #1500

$N_2 > 0$, contact force on specimen can be expected almost constant. This condition of $N_2 > 0$ limits the range of μ values which can be measured by this apparatus. Measured μ is defined as $L/2F_c$ as shown in Fig.3 and applying $N_2 > 0$ to eq.(5) leads to

$$\mu < \frac{sin\theta + \mu_w cos\theta}{cos\theta - \mu_w sin\theta} \tag{7}$$

If μ_w equals 0 the right side of eq.(7) is identical to $tan\theta$. Since the present wedge angel is 15 °, $tan\theta$ becomes 0.268. If μ_w is 0.06 as written in the product manual, the right side of eq.(7) is bellow 0.333. To verify the above consideration, the contact force of hydraulic wedge grip is tried to be monitored under the cyclic axial load in the same frequency and magnitude as the actual frictional test in this study.

The strain through the thickness direction of of the gripping part of the specimen and applied and axial strain are monitored. The results are partly shown in Fig.4. It is found that the strain in a contact direction changes in nearly 15%. This change supposed to be caused by Poisson's effect of the specimen, which needs further discussion. Regular fluctuation of strain in the thickness direction directly related to axial strain confirms that F_c is stable in a long term cyclic experiment. The pressure of preload chamber is monitored through pressure gauge by eye, no change is recognized regardless of the variation of axial load.

Specimen Materials

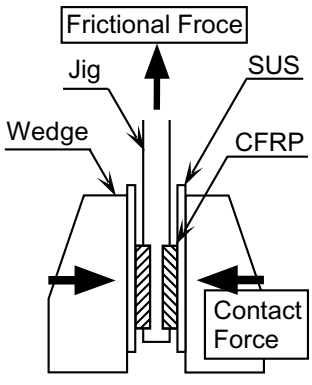

Fig. 5 Scheme of friction test

Unidirectional CFRP is made by T800H/#3631 of Toray. It is cured at 180°C and cut by a diamond cutter into rectangular specimens (25 × 3 × 4 mm) of the fiber volume fraction of 62% with different fiber orientations α. As a counter part material of friction, flat JIS SUS314 stainless steel of 3mm thick is selected and also cut into rectangular specimens (50 × 50 × 3 mm).

The scheme of this frictional test is shown in Fig.5. Two CFRP specimens are embedded into a metal holder on its each side. This holder is sandwiched by two SUS plates with four CFRP specimens embedded. The upper edge of the holder is gripped by the upper grip of test machine, and the frictional force is given by pulling down the lower grip.

Four batches of specimens are tested. In one batch of experiments, fiber orientations are varied as 0°, 30°, 45°, 60°, 75° and 90° for every three pressure, which is 150MPa, 225MPa and 375MPa. From a single experiment for which fiber

orientation α', two data for both α' and 180-α' were obtained because a CFRP specimen moves back and forth on a SUS plate. For later discussion, fiber orientation α is defined as follows. At α<90° fibers stroke the SUS plate and at α>90° fiber tend to stick in the SUS plate. Cycle number N and surface treatment are different in each batch as shown in table 1. Relative speed of 0.2 mm/s, amplitude stroke of 4mm, and room temperature are the same for all.

RESULT AND DISCUSSION

Typical μ-stroke and μ-N curves are shown in Figs.6 and 7 respectively. The μ is defined as $L/2F_c$ at each moment. In Fig.6, each line corresponds to one cycle of μ-stroke curve. In Fig.7 each point corresponds to μ at each moment. As can be seen from them, μ shows monotonic increase with N although a small range of decrease can be recognized in fewer cases especially for α around 90°. In initial part of μ-stroke line μ rises linearly or nonlinearly until it becomes constant. Those curves show a variety of shapes depending on the various conditions of an individual test. Thus, μ_N for N cycle is calculated as an average of relatively stable μ values at the remaining segment of the stroke. First, a line is determined from data sampled within 0.5 second of each cycle by the least mean square method. Next, another line with 90% slope is shown in the μ-stroke sheet. The stable μ is defined as μ less than the 90% slope line. Friction force is influenced by the probabilistic failure of CFRP and relatively stable μ in remaining segment of stroke is also probabilistic and may be different from other batch cases. Therefore μ_N are obtained after averaging between batches and plotted against α.

The distributions of μ_N as a function of α are shown in Figs.8 to 10 for 150MPa, 225MPa and 375MPa, respectively for variations N. Because μ_N almost monotonously increases with N, upper lines approximately corresponds to larger N. The μ_N for $N < 14$ in red, $15 \leq N < 49$ in green and $50 \leq N < 14$ in blue are obtained from 1 to 4, 1 to 3 and 2 to 3 batches. The μ_N is higher for around 90° of α for almost all Pc and N. This seems to be caused by the abrasion of SUS by carbon fiber. As can be predicted intuitively, due to fiber failure at higher P_c this dependency is reduced and α effects are suppressed. At α=0°, μ seems to present different behavior from other μ angle cases. Though CFRP hardly has uniform stress distributions at α of around 90°, at α=0° the stress distribution seems to be relatively uniform. Moreover, at α=0°, carbon fiber is easily worn out. Therefore, the mechanism of monotonous increasing of μ_N is discussed separately at α=0° and 90°.

Frictional behavior at $\alpha = 0°$

At α=0°, the friction behavior of CFRP on SUS seems to be singular, because it becomes easy for a fiber to be worn and separated from the matrix. And due to the effective low modulus of CFRP in a contact of direction, a CFRP specimen uniformly contacts with SUS in a larger apparent area. Therefore, locally high pressures much higher than apparent pressure P_c do not appear so much. The adhesion of SUS to CFRP and accumulation of worn particles of CFRP in a form of film or bulk are not observed either. However, the drop out of fibers from epoxy resin is impressive. As is shown in Fig.13, at higher N and larger P_c the carbon fiber fraction on the frictional surface area is considerably decreased. Therefore, the μ of CFRP is assumed to approach a coefficient of friction of epoxy resin.

The relationship between μ_N and the epoxy resin fraction on the surface area is discussed. The fiber surface fraction of CFRP is measured and the rule of mixture is applied to μ_N. Optical microscopic photographs are taken at two specific points of each CFRP specimen. Four CFRP

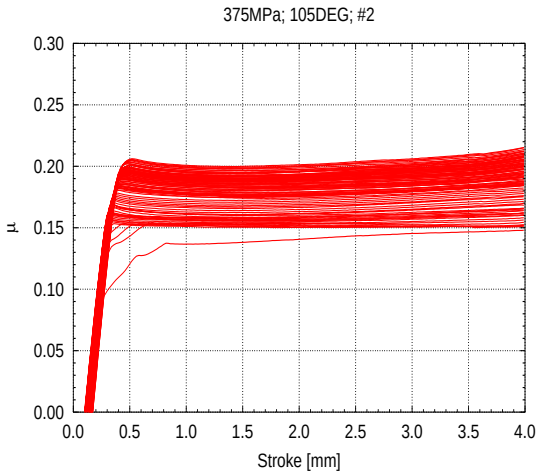

Fig. 6 μ-stroke curves

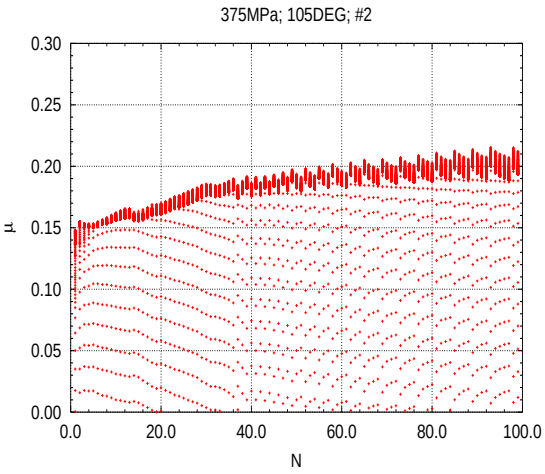

Fig. 7 μ-cycle curves

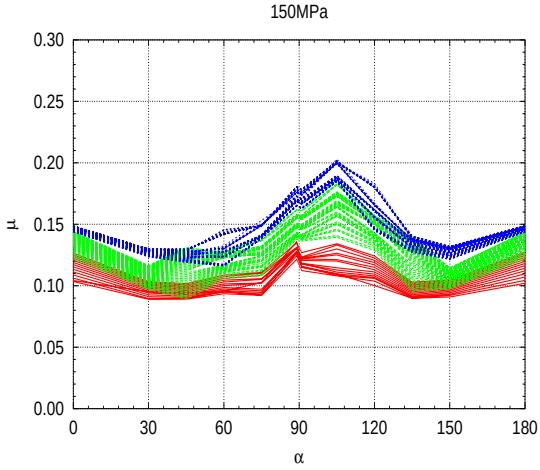

Fig. 8 μ distribution with α

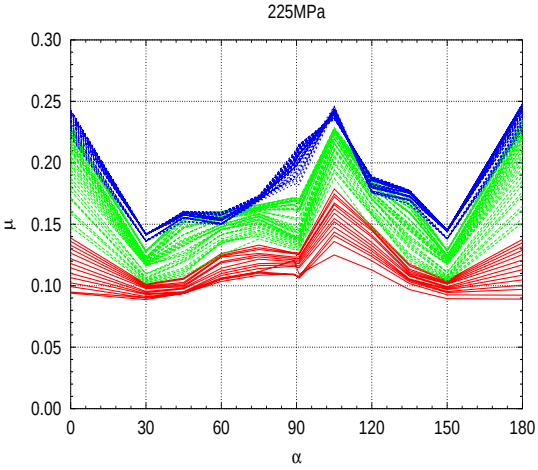

Fig. 9 μ distribution with α

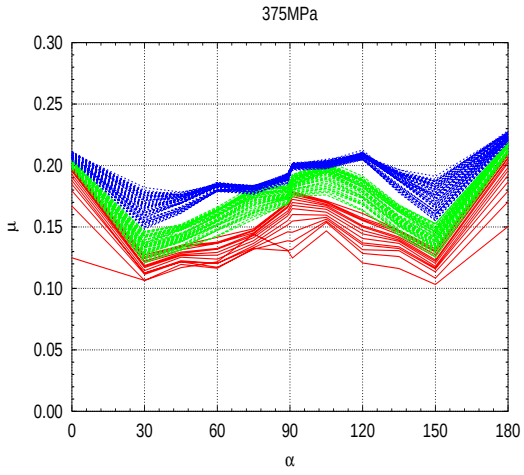

Fig. 10 μ distribution with α

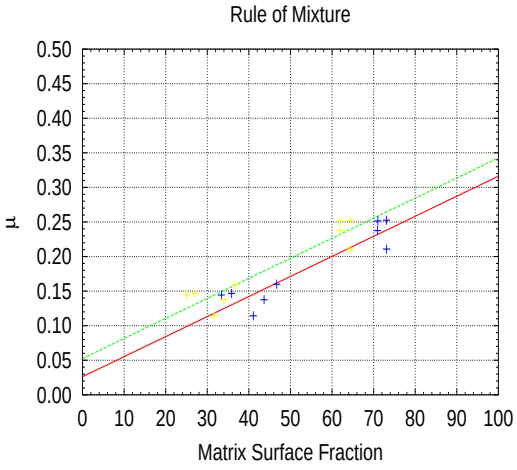

Fig. 11 Rule of Mixture

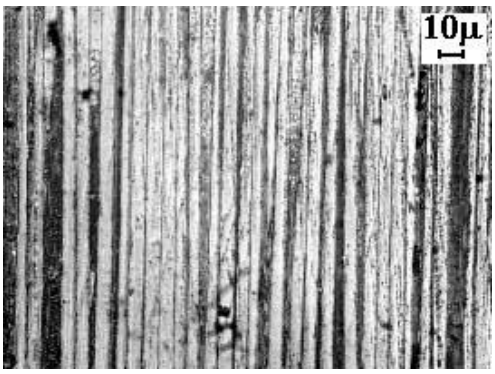

Fig. 12 0° CFRP;133MPa;50cycles

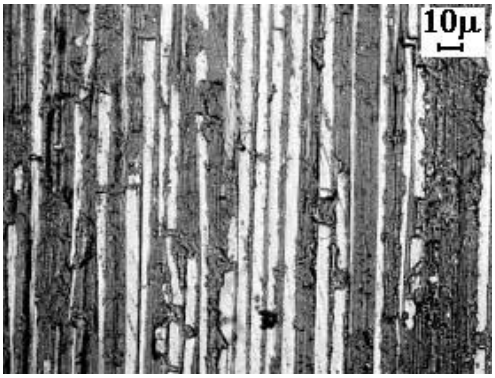

Fig. 13 0° CFRP;200MPa;50cycles

specimens are used for one cases and 0.4% of the whole frictional surface is measured. Fiber region is shown in rather white. Those micro photographs are scanned into a PC and each segment of the image is decided to be fiber or epoxy by applying an appropriate threshold value to the segment data.

At first, μ_F and μ_M are calculated applying the rule of Mixture. Here, μ_F and μ_M represent the coefficients of friction of carbon fiber and epoxy, respectively. Measured matrix and fiber areas are presented as s_M and s_F, respectively. Then, the matrix area fraction f_M is simply defined as

$$f_M = \frac{s_M}{s_M + s_F}. \tag{8}$$

$$\tag{9}$$

In this case as can be seen in Fig.11, $\mu_F = 0.026$ and $\mu_M = 0.316$. These values are different from known data under a typical pressure. Therefore, instead of f_M an equivalent matrix fraction is defined as

$$s_M^* = w_M s_M, \tag{10}$$

$$s_F^* = w_F s_F, \tag{11}$$

$$f_M^* = \frac{s_M^*}{s_M^* + s_F^*}, \tag{12}$$

where w_M and w_F are the weights of each component, which take into account their modulus in a contact direction. Both w_M and w_F are calculated by FEM using a simple model, where CFRP including a single fiber or matrix corresponding to several fibers on the CFRP surface is compressed with uniform displacement. They are obtained as $w_M = 0.825$ and $w_F = 1.24$ in this case. Then, $\mu_F = 0.053$ and $\mu_M = 0.343$ are calculated as shown in Fig.11. This values seem to be more reliable than those aforementioned.

Frictional behavior at $\alpha \neq 0°$

There is a peak of μ_N at α little over than 90°. This distribution of μ_N with α seems to be the result of abrasion occurred on a frictional surface. From the microscopic point of view, there must be a stress concentration at a fiber edge on a frictional surface, where a fiber can penetrate into the SUS surface and abrade it. Moreover, for α closer to 90°, the Young's modulus of fiber

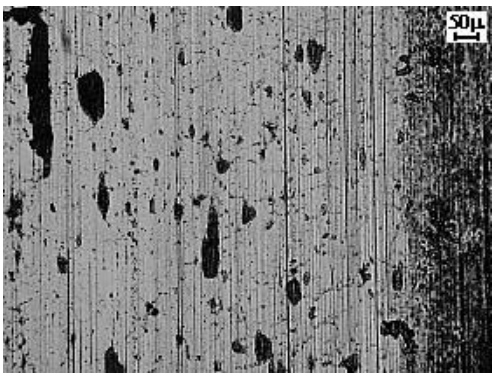

Fig. 14 75° CFRP;200MPa;100cycles

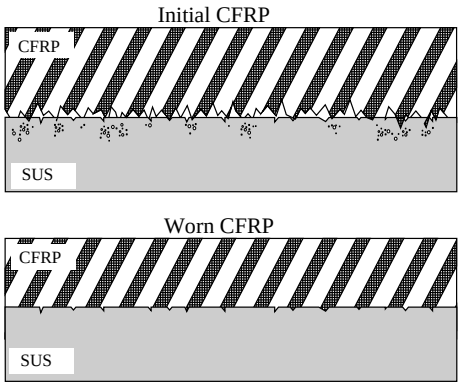

Fig. 15 CFRP surface morphology

in a contact direction become large. Then, the distribution of contact pressure on the frictional surface becomes less uniform according to a contact condition. This irregularity cannot be prevented in this friction. By these reasons, at α closer to 90°, SUS is abraded more by fibers. This abrasion results in higher μ_N. For the 90° CFRP, considerable adhesion of SUS can be seen even for at relatively low pressure and small N, although the adhesion of SUS increases with N and P_c in general.

In addition to the adhesion of SUS on a CFRP specimen, the accumulation of worn particles are also observed under the severe abrasive condition. These worn particles seem to consist of CFRP and SUS. Their morphology change, according to the degree of abrasion. For relatively low N and P_c it looks powdery and forms a thin layer over CFRP. However, for large N and/or high P_c, it becomes solidly rather than powdery and forms a rather thick layer. Under a further severe condition it has a glossy appearance, which looks to be once melted and coagulated as shown in Fig.14. This glossy substance also adheres to the SUS surface, too. Then, the friction no longer takes place between SUS and CFRP, but it takes place between the same substances. Generally it is known that the friction between the same substances is large. Therefore, increase of this type of frictional area between the same substances can cause an increase of μ_N as shown in Figs.8 to 10. The slight increase of μ_N with P_c can be understood from the same principle. That is, at higher P_c, the larger frictional area between the same substances appears and makes μ_N increase.

For small N, the distribution of μ_N is rather uniform and the strong dependency on the fiber orientation cannot be recognized. This is because in the initial cycle, there exist many microscopic asperities on the CFRP surface which are easily worn out by small shear stress. Fig.15 illustrates this schematically. By turning these asperities into rolling particles, specimens can slide easily and μ_N becomes relatively small. Furthermore, μ_N stays rather independent of α until asperities have worn out. At P_c=375MPa, μ_N does not depend on α, either. It seems to be that a fiber fails under a high pressure and α does not have much effect on the friction.

EPMA Observation

EPMA mapping and SEM images are shown, in Figs.16 to 19 with five images in each figure. A SEM image is in the center and others display intensities of elements, S, Fe, (SEM,) O and C from left to right. SEM images of Fig.16 and Fig.17 show SUS and CFRP surface, respectively, which have the similar appearance to the other. In this area, it is thought that the

same substances adhere on both surface and μ_N takes a relatively high value. The intensity of O is very high at the same place as Fe. This means that that during cyclic friction, Fe is gradually oxidized. This oxidization seems to be caused by a locally high temperature produced by the frictional work. By comparing Figs.17 and 18, it can be seen that oxidization increases with N. In Fig.18 of N=15, although accumulation of SUS on a CFRP surface is approximately similar to the Fig.17 case, a relatively rough surface suggested by SEM images indicates lower μ_N at small N. Comparison of Figs.17 and 19 shows the effect of α on the friction. Clearly at α=45 °, less SUS is abraded and slight oxidization is recognized. Strong intensity of carbon in Fig.19 indicates that the film layer which covers the CFRP surface is thin. This is also imagined from the SEM image.

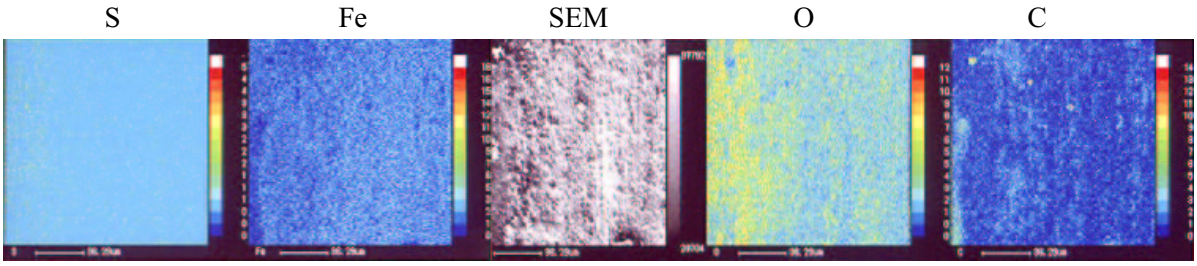

Fig. 16 90° SUS; 333MPa; 100cycles

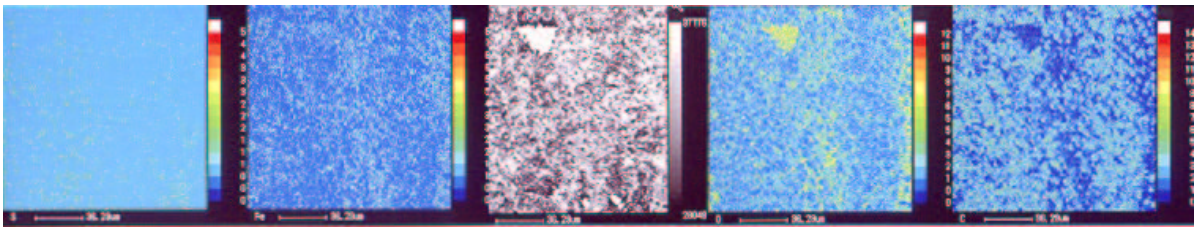

Fig. 17 90° CFRP; 333MPa; 100cycles

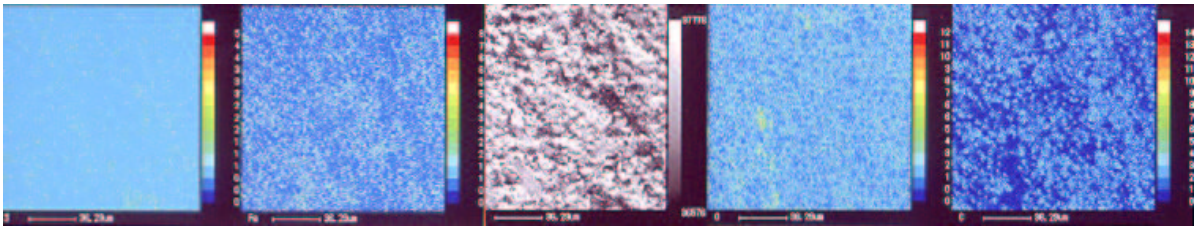

Fig. 18 90° CFRP; 333MPa; 15cycles

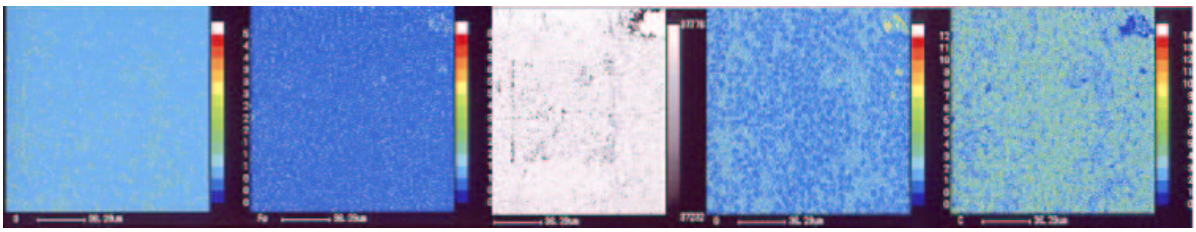

Fig. 19 45° CFRP; 333MPa; 100cycles

CONCLUSION

In this study, the coefficient of friction between CFRP and SUS under a critically high contact pressure are investigated. The followings can be pointed out as conclusions.

- An apparatus for the frictional experiment under a high contact pressure is designed and its validity is verified.
- The coefficient of friction are obtained with contact pressure, fiber orientation and reciprocation number as parameters.
- The coefficient of friction shows the maximum at the fiber angle α a little over than 90 $^\circ$ due to the effect of abrasion by fiber.
- Coefficients of friction increase with reciprocation number almost monotonously at every fiber orientation.
- The mechanism is different between the 0° CFRP and the other cases. For α=0° it is caused by the increase of epoxy area fraction on a CFRP surface. For the other angles it is caused by the adhesion of a substance, which is made of worn out CFRP and SUS, on both surfaces.
- A high contact pressure suppresses the effects of fiber orientation. The coefficient of friction becomes higher under a higher contact pressure.
- EPMA mapping analysis of specimens supports above mentioned several explanations.

REFERENCES

1. F.L., Mattews (ed.,), Joining Fiber-Reinforced Plastics, Elsevier, (1986).
2. T.Tukizoe and N.Ohmae, Friction and wear of polymer composites, ed. K.Friedrich, Vol. 1, ch7, (Elsevier, Amsterdam),p.p205-231(1986).
3. Y. Xiao, Effect of Carbon Fiber Direction of Unidirectionally Reinforced Epoxy Composites on Frictional Behavior, Journal of the society of materials science Japan Vol.47, No.6, pp.618-624, June, (1998)
4. Y. Xiao, W. X. Wang and Y. Takao, Bulletin of Research Institute for Applied Mechanics Kyushu University Vol.82, pp167-178
5. MTS Systems Corporation, MTS Product Information, January (1996).
6. Japanese Society of tribologist,Tribology of new material,Yokendo LTD. (1991).
7. Ed. Klaus Friedrich, Friction and wear of polymer composites, Composite Materials Series Vol.1 Elsevier,1986